SPECTRUM AVERAGING IN A MIMO FMCW MARITIME RADAR FOR A SMALL FLUCTUATING TARGET RANGE ESTIMATION

SURAYA ZAINUDDIN[1], NUR EMILEEN ABD. RASHID[2,*],
IDNIN PASYA IBRAHIM[2], RAJA SYAMSUL AZMIR RAJA ABDULLAH[3],
ZUHANI ISMAIL KHAN[2]

[1]Fakulti Teknologi Kejuruteraan Elektrikal dan Elektronik, Universiti Teknikal Malaysia Melaka, 75450, Ayer Keroh, Melaka, Malaysia
[2]Microwave Research Institute, Universiti Teknologi MARA, 40450, Shah Alam, Selangor, Malaysia
[3]Faculty of Engineering, Universiti Putra Malaysia, 43400, Serdang, Selangor, Malaysia
*Corresponding Author: emileen98@uitm.edu.my

Abstract

Detection of a small maritime target has been challenging in radar signal processing due to the object size near the water surface. This paper provides an alternative detection method for a small fluctuating target by deploying a frequency modulated continuous waveform (FMCW) in a multiple-input multiple-output (MIMO) configuration. The work proposed a MIMO FMCW radar with a frequency offset between transmitted sub-bands, and the spectrum averaging (SA) scheme to combine the multiple received signals. A MIMO with an equal number of transmit and receive nodes were employed, and transceivers were co-located. The frequency-offset introduced an interval band between MIMO sub-signals to avoid interference and overlapping. The work observed range error parameters of a small fluctuating target. The result reveals that applying the SA with and without an interval band produced a better performance against signal-to-noise ratio (SNR) in terms of probability of range error and range error mean, through numerical simulations and experiments. However, MIMO caused an incremental computational complexity with the number of nodes based on Fast Fourier Transform (FFT) algorithm.

Keywords: Fluctuating, FMCW, Maritime, MIMO, Multi-frequency, Radar, Spectrum averaging, Swerling.

1. Introduction

Commonly, a standard vessel tracking system is meant to detect long-distance commercial vessels with a huge size [1] and is not suitable for small targets such as small fisherman boats. Therefore, radars mounted on vessels were utilised as a complement for small targets detection. These radars are known for their reliability; however, target detection is limited to single-radar coverage without redundancy or backup. Furthermore, due to clutter by the water surface and target's low-profile characteristics, detecting a small fluctuating target is still an issue to mitigate.

A small maritime target radar cross-section (RCS) can be presented by the Swerling 1 model, which indicates a slow RCS changing that is independent from scan-to-scan [2-4]. A fluctuating RCS increases the difficulties in small targets detection. Reference [5] examined in detail maritime fluctuating targets.

Various methods have been introduced to the issue through radar configurations, waveform design and processing algorithms. In recent works, radar configurations such as multi-static and forward scatter radars had been experimented [6]. Besides, utilisation such as photonics-based radar [7, 8], synthetic aperture radar (SAR) [9, 10] and digital versatile broadcasting - television (DVB-T) passive radar [11] had proven to enhance detection of maritime targets. Furthermore, radar placement such as space-borne [9, 10, 12] and vessel-mounted [11, 13, 14] had been studied to provide better spatial coverage and flexibility to the system.

Evolution in radar configuration presents a multiple-input multiple-output (MIMO) radar which promises significant improvements over conventional configurations, such as single-input single-output (SISO) [15]. In this paper, MIMO was applied with a frequency modulated continuous waveform (FMCW), which offers energy efficiency and yields a better signal-to-noise ratio (SNR) [16]. Furthermore, an FMCW is also favoured in the maritime environment as it provides a better range resolution. Several concepts of FMCW over a MIMO configuration had been reviewed by Hinz and Zölzer [1], but the range estimation performance of each scheme proposed was not discussed. Various MIMO-FMCW approaches were studied, such as the reference [17], which utilised different polarities with limited freedom.

A convergence of MIMO configuration and frequency modulation scheme had been studied in reference [18, 19] to improve the target range estimation. Frischen et al. [20] discussed the MIMO linear FMCW performance of range error parameters over SNR by applying a monostatic-bistatic distance measurement for a non-fluctuating target with different parameters studied by this paper. Meanwhile, Noor et al. [19] simulated a small Swerling 1 target and presented a better probability of range error performance by applying a beat averaging in a time domain. However, it was unable to compare the performance because a different target range was utilised, and target RCS was slightly higher.

Thus, this study provides a promising alternative approach to detect a small target with a slow-fluctuating characteristic, by applying a MIMO with multi-frequency triangular FMCW. This work also contributes to the receiver's fusion scheme by using spectrum averaging (SA). A signal averaging technique is commonly performed over a repetitive signal from a single source to recover the signal out of the noise. Hence, the idea was to use SA to form a spectrum

accumulation of MIMO beat signals. This research was conducted on independent MIMO nodes with an equal number of transmitting and receiving antennas through numerical simulation and experiment. Experiments used a commercial-off-the-shelf (COTS) module to accelerate MIMO configuration development, namely Distance2go (D2G). However, the challenge of implementing the COTS includes the limitation of transmitting power, fixed sampling points and frequency range. Overall, using multi-frequency MIMO with an interval band and the SA scheme improved the range error performance for a small and slow-fluctuating target.

The proposed method is explained in Section 2, followed by the numerical simulation results in Section 3. Next, the experimental validation is presented in Section 4, and finally concluded in Section 5.

2. The Proposed Methods

The work proposed a MIMO configuration utilising multiple FMCW sub-bands at different frequency ranges to estimate the range for a small slow fluctuating target. This paper discusses a MIMO radar consists of M transmitting and N receiving antennas, to detect a target at a distance R. The proposed SA scheme was applied at the receiver to combine multiple received signals by averaging Fast Fourier Transform (FFT) spectrums.

As mentioned prior, signal averaging or signal recovery technique is usually applied over a repetitive signal obscure by noises. This technique exploits similar information embedded in received signals. The concept was employed by averaging the FFT of beat signal spectrums from N MIMO nodes. Spectrums were accumulated, and magnitudes at each FFT point were averaged. The spectrum resulted from the averaging is possible to extract the coherent response reflected by a target. In addition, a frequency interval was introduced to lessen interference and overlapping effects by neighbouring signals. However, this method required synchronisation between each MIMO sub-bands.

Figure 1 illustrates an example of a 2×2 MIMO FMCW radar with SA implementation. $M = 2$ and $N = 2$ with a target distance of 50 m were simulated. However, the target was measured at 10 m during experiments due to hardware transmit power limitation. As per Fig. 1, the configuration consisted of two transmit antennas (TX_1 and TX_2) and two receive antennas (RX_1 and RX_2).

There were two chirp generators for a 2×2 MIMO setup, which generated baseband at two frequency ranges. The carrier frequency modulated each baseband for the independent antenna to emit. A target at R distance reflected transmit signals and echoes received by both antennas. Signals were propagated over a free-space path loss (FSPL). Received signals acquired by a receiver were demodulated to baseband and filtered by a bandpass filter for sub-band processing and noise suppression. For simulation, Hamming finite impulse response (FIR) filter with a 100th order was utilised to obtain a narrower transition band. Each filtered signal was mixed with the reference signal in a time domain to produce a beat signal.

Next, the beat signal was applied with Fast Fourier Transform (FFT) algorithm, and the FFT spectrum was input into the proposed SA block. For a 2×2 configuration, the SA gathered four frequency spectrums and averaged the magnitude at each sample point. It resulted in a single spectrum at the output and obtained the local maxima peak for positive and negative regions by applying peak detection. These peaks were utilised for target range estimation.
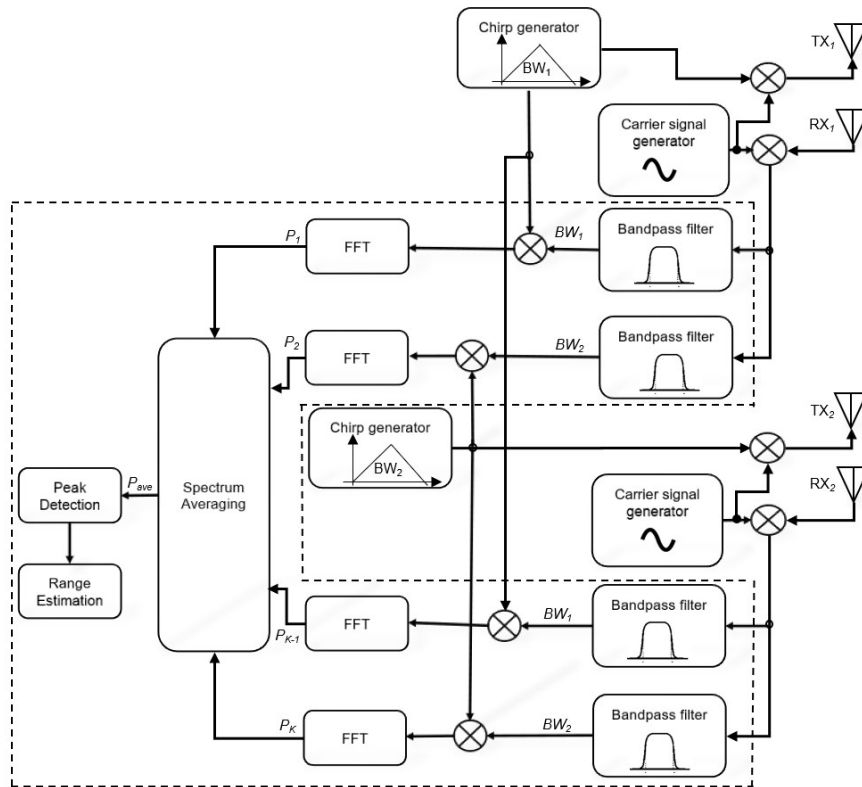
Fig. 1. Block diagram of a 2×2 MIMO FMCW radar.

2.1. Spectrum averaging for received signal fusion

In the setup, a MIMO radar emitted multiple signals from multiple antennas. Hence, the proposed method of spectrum averaging was applied at the receiver to combine these received signals. In Fig. 1, blocks surrounded by the dashed line presents 2×2 MIMO FMCW radar receiver processing. The SA averaged all FFT spectrums into a single spectrum which the output magnitude, P_k, can be defined by

$$P_{ave} = \frac{1}{K}\sum_{k=1}^{K} P_k(f) \tag{1}$$

With $K = M \times N$. While k indicates the number of FFT output. By taking a 2×2 MIMO as an example, the FFT spectrums can be presented as the log magnitude of P_1, P_2, P_3 and P_4 with $K=4$. By utilising Eq. (1), P_{ave}, can be written as

$$P_{ave} = \frac{1}{4}\sum_{k=1}^{4} P_1(f) + P_2(f) + P_3(f) + P_4(f) \tag{2}$$

Next, the spectrum's peak detection algorithm was performed to obtain the local maxima for range estimation. Finally, the beat frequency, f_b, was utilised in Eq. (3) to estimate the range of a target. Denotes that c is a constant for the velocity of light, T is the sweep period and B is the sweep bandwidth.

$$R_{est} = \frac{cTf_b}{4B} \tag{3}$$

2.2. Interval band implementation between MIMO sub-bands

Next, the interval band was proposed to avoid overlapping and interference between sub-bands as Fig. 2. Independent chirp generators generated each sub-band at a different frequency, and each was emitted by an independent antenna.
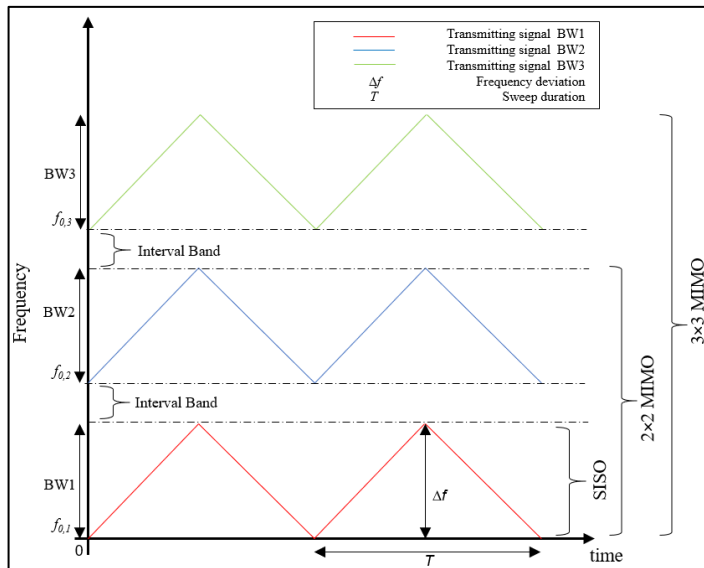

Fig. 2. The proposed MIMO FMCW transmit sub-bands.

A 10 MHz sweep bandwidth was utilised for numerical simulations, and a 20 MHz sweep bandwidth was utilised for experimental analysis, equivalent to 15 m and 7.5 m range resolution, respectively. Sweep bandwidths were chosen to avoid extensive frequency band usage in a multi-frequency MIMO implementation. However, a larger sweep bandwidth was applied during experiments to compensate for the hardware's FFT point limitation, which resulted in a higher maximum error [21]. The range resolution is given by Eq. (4) with c is the velocity of light and B is a bandwidth.

$$\Delta r = \frac{c}{2B} \tag{4}$$

The accuracy of the range estimation was within a relative difference of ± 7.5 m to the actual target range, for simulation and experiment. The error threshold was configured within the maximum range error given by Eq. (5).

$$\Delta R = \frac{cTf_s}{2BN_s} \tag{5}$$

In which, ΔR is the maximum range estimation error, c is the velocity of light, T is a sweep period, f_s is a sampling frequency, B is a bandwidth and N_s is a number of samples.

This scheme was simulated for a static and a moving target. However, it was evaluated over a static maritime target due to hardware and environmental limitations in the experiment. A 2 MHz interval was adopted to recompense the FIR filter utilised. A narrower transition band can be obtained by a larger filter order for sub-bands isolation. However, a larger order increased a filter delay [22].

The simulation and experiment data were observed against signal-to-noise ratio (SNR) between -6 dB to 30 dB to examine the effect of white Gaussian noise level over the error performance.

This proposed multi-frequency method for MIMO requires a higher bandwidth with the incremental antennas' number. On the other hand, a similar bandwidth utilised for a time-staggered MIMO may results in a better range resolution. However, a time-staggered method requires time offset between elements to be larger than the maximum round trip time, and synchronisation between transmit and receive is crucial [1].

3. Numerical Simulation: Validation and Verification

The influence of the proposed configurations was simulated, and the error performance was analysed. The system was validated through the MIMO received signals, the probability of range error and range error mean. Table 1 tabulates parameters utilised for the simulation.

Table 1. Parameters utilised for the numerical simulation.

Waveform type	Frequency modulated continuous waveform (FMCW) - Triangular
Operating frequency, f_c	1.3 GHz
Sweep bandwidth, B	10 MHz
Sampling frequency, f_s	80 MHz
Number of samples, N_s	16×10^5
Sweep period, T	20 ms
Range resolution	15 m
Target RCS/ range	Swerling 1, 10 m^2/ 50 m
Sub-bands baseband range	
• With 2 MHz interval band	BW1: 0 Hz to 10 MHz
	BW2: 12 MHz to 22 MHz
• Without interval band	BW1: 0 Hz to 10 MHz
	BW2: 10 MHz to 20 MHz
	BW3: 20 MHz to 30 MHz

The simulation was constructed to be able to measure a long-distance target over a wide maritime area. Thus, a practical long-range radar frequency of 1.3 GHz was utilised due to its robustness against noise and weather. For this scenario, the target was configured at 50 m. 10 MHz bandwidth was opted to obtain a 15 m range resolution to suit the simulated distance. The 80 MHz sampling frequency was to cater the bandwidth utilisation up to a 3×3 MIMO configuration. In the interval band simulation, a static and a moving target were evaluated to observe the influence on error parameters.

3.1. Received signal analysis

MIMO received signals were observed in terms of spectrogram and frequency spectrum. There were remaining frequency components that existed for a condition without interval band, as Fig. 3(c). However, the interval band's implementation provided a sufficient gap between sub-bands and resulted in no remaining frequencies appeared after the sub-bands filtering as Fig. 3(d).

Figure 3 depicts the spectrogram of received signals in detecting a small fluctuating target. This spectrogram analysis displayed an energy map but did not reflect the impact of setup over range estimation. There was a slight frequency shifting due to the target motion. However, the change was unnoticeable in the energy map. Thus, the received signal was further examined over its SA's output spectrum as per Fig. 4.

(a)

(b)

2 MHz Interval Band

(c)

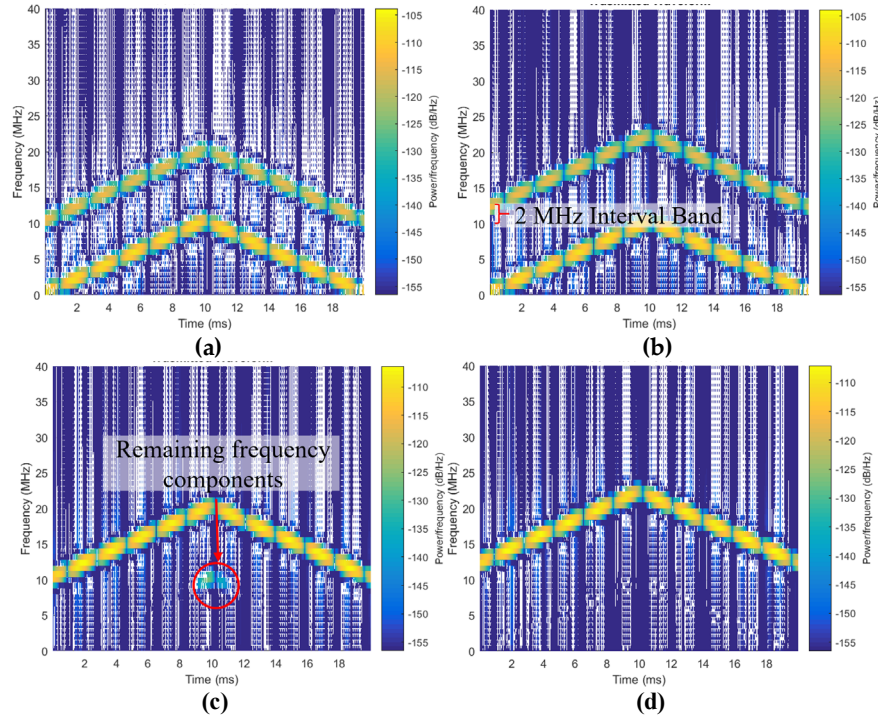Remaining frequency components

(d)

Fig. 3. Spectrogram of a 2×2 MIMO FMCW received baseband signals; (a) without an interval band, (b) with a 2 MHz interval band (the proposed method), (c) filtered BW2 without interval band, and (d) filtered BW2 with an interval band, in detecting a small fluctuating moving target.

Figure 4 depicts an example of the SA spectrum for 2×2 co-located MIMO radar in detecting a small target at SNR = 30 dB. The observation indicated that the maximum beat frequency peak was easily distinct for a static target presented by the blue curve. The static target produced a positive peak at 325 Hz, resulting in an estimated range of 48.75 m. In the static target scenario, only the positive region was utilised for range estimation as in theoretical both regions produce the same peak. However, a moving vessel produced a left-skew spectrum due to the doppler. In addition, moving target spectrums had high-neighbouring peaks, which in the case they overshoot the actual peak, the error may occur. In this example, with and without an interval band configuration produced a similar positive peak at 125 Hz and a negative peak at 625 Hz, resulting in a beat frequency of 375 Hz equivalent to 56.25 m. Even though there was a frequency shifting when detecting a moving target, a multi-frequency FMCW setup produced an acceptable range estimation.
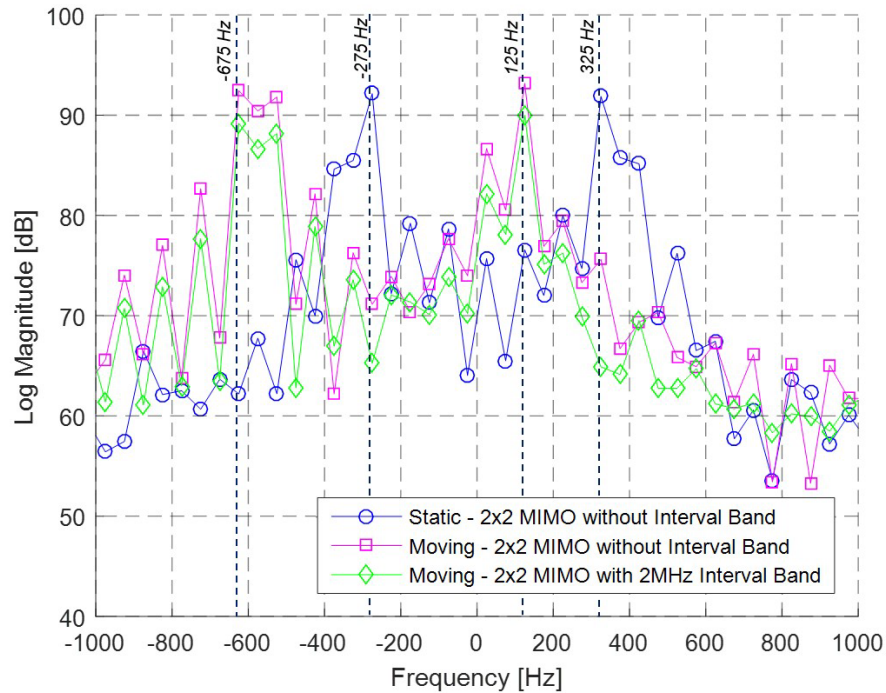
Fig. 4. Frequency spectrums of the SA for 2×2 co-located MIMO FMCW radar in detecting a small fluctuating target at 30 dB SNR.

3.2. The probability of range error and the range error mean

The range error performance was further evaluated regarding the probability of range error and range error mean, against the SNR. The impact of SNR level on system performance was observed by adding the additive white gaussian noise (AWGN) to receiver nodes. The SNR quality was varied to measure the capability of the proposed method. It was evaluated for 10,000 runs to ensure the statistical behaviour of the simulated system. These performance analyses observed the influence of noise on the accuracy and robustness of target range estimation.

The probability of range error represents the system's robustness to produce the right decision concerning the error level. Meanwhile, the range error mean provides a view of estimation accuracy. Range error was classified as any estimation which differs more than 7.5 m from the actual range, which was within the maximum range error.

3.2.1. The effect of a MIMO FMCW with spectrum averaging implementation

In this simulation, a 2×2 co-located MIMO was observed against a SISO as Fig. 5. Region 2 depicts a MIMO with the proposed spectrum averaging outperforming a SISO, as it enhanced the signal energy by combining multiple received MIMO signals. However, a MIMO signal energy was submerged by noise from multiple sources at lower SNR in region 1 and resulted in performance degradation compared to SISO.

A MIMO achieves the 20% probability of range error at 8.6 dB, which is 0.85 dB better than a SISO configuration. It displays that the proposed MIMO configuration is more reliable in producing range estimation at slightly lower SNR. The comparison was taken at the 20% error probability as the detection probability in a Gaussian noise environment occurs between 75% to 95%. A MIMO setup also produces average error readings within the 7.5 m threshold begins at 29.5 dB, while SISO is still encountering a higher error until 30 dB. Both configurations reach the 0% probability of error at more than 30 dB SNR. From the range error mean curves, it was discovered that the system accuracy increased with the improvement of SNR, and better accuracy can be achieved through the proposed scheme. Both curves produced a high error mean at lower SNR due to high FFT points utilised in simulation across the 10 MHz bandwidth. This behaviour can be observed through all simulation results.
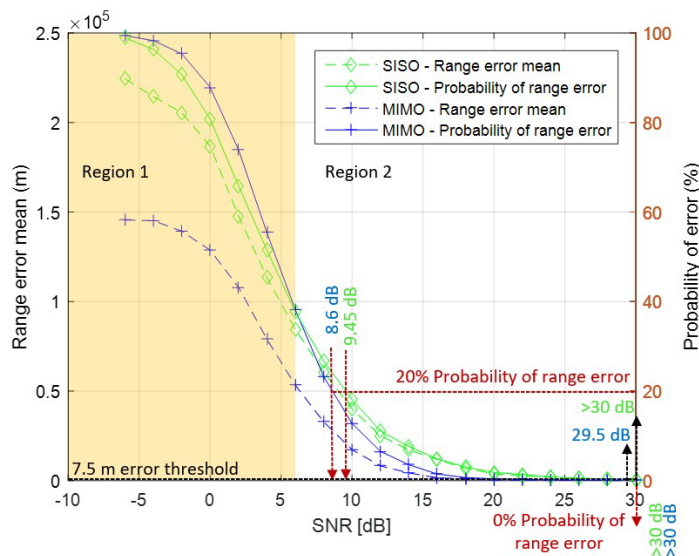

Fig. 5. The effect of a MIMO FMCW with spectrum averaging scheme implementation.

3.2.2. The effect of larger MIMO FMCW configuration

Next, the effect of implementing more nodes in MIMO configuration was evaluated by introducing additional nodes to form a co-located 3×3 MIMO. Figure 6 shows that a 2×2 co-located MIMO slightly surpasses a 3×3 co-located MIMO in region 1 for the probability of range error due to a lesser source of the noise. However, a setup with more nodes starts to outperform a setup with lesser nodes in region 2, benefiting from the SA implementation. It indicated that more signal spectrums fuse to the SA produced a better detection accuracy and reduced estimation error. Besides, a MIMO system also offers redundancy for backup with more nodes.

A 3×3 MIMO reaches the 20% probability of range error at 7.72 dB and follows by a 2×2 MIMO at 8.6 dB. Both configurations produce the 0% probability of error at more than 30 dB. For a range error mean parameter, a setup with more and a setup with lesser nodes achieve the allowable threshold, beginning at 22 dB and 29.5 dB, respectively. A setup with more nodes was producing a better average range error throughout the SNR.
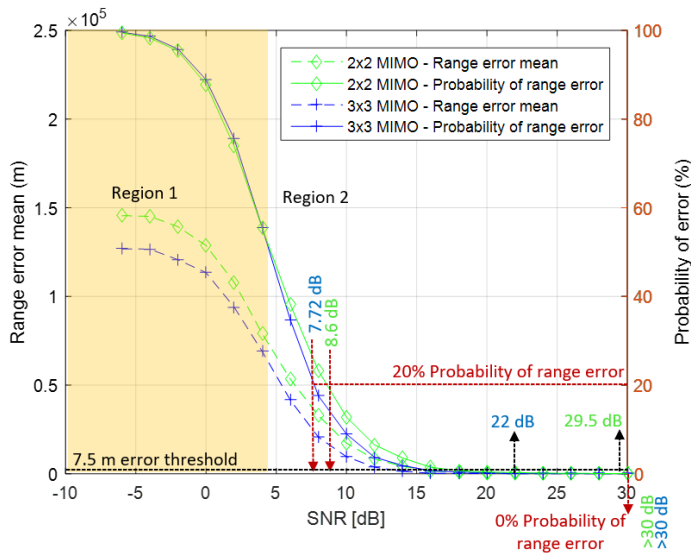
Fig. 6. The effect of more MIMO node configuration.

3.2.3. The effect of an interval band implementation

A frequency shift by a target motion has been presented previously in Fig. 4. Thus, the interval band between MIMO sub-bands was proposed to prevent overlapping between neighbouring bands, moreover when shifting occurred. A 2 MHz gap was introduced to match the 100th filter order. The high filter order was utilised for a narrow transition band for a better selectivity of the required signal. However, the bandgap was chosen with consideration of the filter delay.

Figure 7 presents the probability of range error and range error mean using a 2×2 MIMO configuration to detect a static target. The graph with interval band implementation surpasses the setup without interval band for 2.4 dB in achieving the 20% probability of range error. By applying an interval band in the setup, the 20% probability was achieved at 6.2 dB.

On the other hand, a similar performance was achieved by non-interval at 8.6 dB. Besides, the setup with frequency gap produced 0% probability error at 28 dB and the other configuration was still producing error at 30 dB. The same trend is observed from the range error mean graph, with the blue dotted curve outperforms the green dotted graph. The blue curve reaches an error below 7.5 m at 26 dB, while the green curve at 29.5 dB. These results indicate the advantage of having the interval band.

Next, Fig. 8 depicts the probability of range error and range error mean, without and with the interval band for a moving target. However, the results were remarkably close to each other. The interval band's implementation achieved the 20% range error probability of 0.08 dB earlier than the non-interval band setup, at 9.14 dB. However, the configuration applying both schemes produced the 0% error at 30 dB, and a setup without interval still had errors at this SNR level. In addition, both setups delivered the acceptable error mean at the 30 dB, with a non-interval band resulting in a higher error. It was observed that the range error mean for both fluctuated between 24 dB to 30 dB.
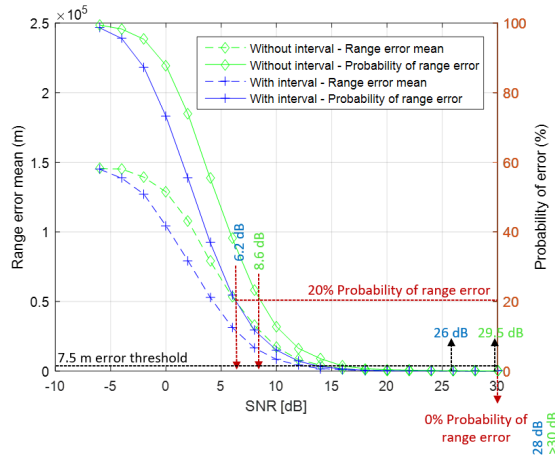
**Fig. 7. The effects of 2 MHz interval band
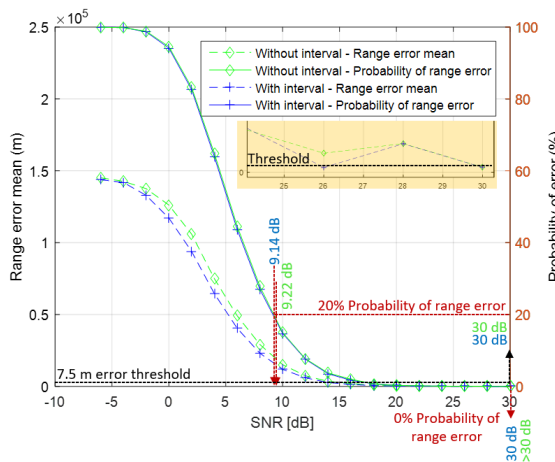implementation for a static target estimation.**

**Fig. 8. The effects of 2 MHz interval band
implementation for a moving target estimation.**

The influence of frequency interval between MIMO sub-bands using FMCW
was demonstrated to reduce the error performance of the simulated system. Even
though the result of the moving target shows a slight improvement, the setup with
interval displayed a more stable estimation than the other.

3.3. Computational complexity

An algorithm performance can be assessed its efficiency through time, space and
energy cost [23]. In this paper, the time cost was evaluated regarding FFT [24]
algorithm as the proposed method involved massive utilisation of FFT with
incremental nodes. The algorithm is presented in O-notation as follows.

$$O(MNS \log_{10} S) \tag{6}$$

M is the number of transmitting nodes, N is the number of receive nodes and number
of samples, S. Table 2 summarises overall simulation performance and a simple
operational complexity calculation with regards to FFT, in the case of $S = 256$.

Table 2. Comparison between simulated configurations.

Configuration	Probability of Range Error = 20%	Probability of Range Error = 0%	Range Error Mean	Computational Complexity
Target motion = static				
SISO	9.45 dB	> 30 dB	> 30 dB	O (617)
22 MIMO with SA	8.6 dB	> 30 dB	29.5 dB	O (2466)
3×3 MIMO with SA	7.72 dB	> 30 dB	22 dB	O (5549)
2×2 MIMO with SA & interval	6.2 dB	28 dB	26 dB	O (2466)
Target motion = moving				
2×2 MIMO with SA	9.22 dB	> 30 dB	30 dB	O (2466)
2×2 MIMO with SA & interval	9.14 dB	30 dB	30 dB	O (2466)

In Table 2, the incremental complexity is clearly seen with the expansion of MIMO nodes, which increased FFT time processing. However, error performance was improved. Besides, the SA application over MIMO beat signals processing and interval band between sub-bands were proven to produce better results.

4. Experimental Validation: Results and Discussion

Finally, the performance of the proposed scheme was verified through experiments. Experiments were conducted to detect a small fluctuating target over a lake surface. A D2G module by Infineon has limitations on its transmit power, transmit frequency range, sweep period and number of sample points. Therefore, the target range was configured at 10 m to suit the D2G transmit power capability. Parameters utilised during experiments differed based on support by the hardware, and 1,000 data sets were acquired. Table 3 tabulates parameters applied for experiments.

Table 3. Parameters utilised for the experiment.

Waveform type	Frequency modulated continuous waveform (FMCW) - Triangular
Sweep bandwidth, *B*	20 MHz
Sampling frequency, *f_s*	640 kHz
Number of samples, *N_s*	256
Sweep period, *T*	0.4 ms
Range resolution	7.5 m
Target environment	Lake, with small ripples
Target range	10 m
Target motion	Static
Sub-bands sweep frequency range	
• **With 2 MHz interval band**	BW1: 24.025 GHz to 24.045 GHz
	BW2: 24.047 GHz to 24.067 GHz
	BW3: 24.069 GHz to 24.089 GHz
• **Without interval band**	BW1: 24.025 GHz to 24.045 GHz
	BW2: 24.045 GHz to 24.065 GHz

Figure 9 depicts the experiment setup. Radar under tests (RUTs) was mounted over 2 m height polyvinyl chloride (PVC) pole fixed at the lake's bank to reduce the land propagation effect. In addition, a 1 m height target was covered with aluminium foil with reflectors mounted on it. All experiments were carried out to estimate the range of a static target which was placed on a float at 10 m from transceivers.
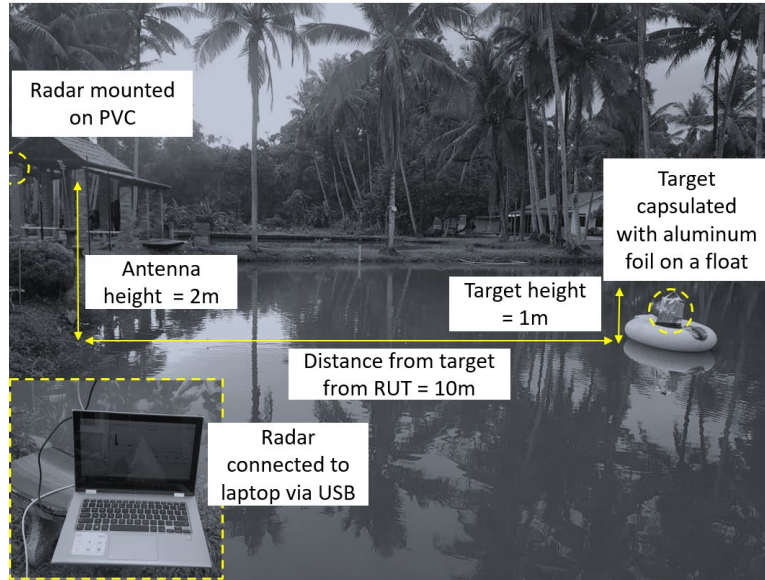

Fig. 9. A view of the outdoor measurement
setup for detecting a small static, slow fluctuating target.

The probability of range error and the range error mean

Experiments were conducted to verify the range error performance for the probability of error and range error mean. In experiments, beat signals from D2Gs were post-processed in MATLAB. Each beat signal in a time domain was added with AWGN at the desired SNR and applied with the FFT algorithm. The signal processing was similar to simulation.

4.1. The effect of a MIMO FMCW with spectrum averaging implementation

Firstly, a 2×2 MIMO FMCW applying SA without interval band configuration was analysed. The setup was observed to surpass a SISO across the SNR, as Fig. 10. A MIMO produced the 20% probability of range error at 12.25 dB, while a SISO produced a similar performance at 17.2 dB. The proposed setup delivered the 0% error probability at 20 dB, 8 dB earlier than the conventional SISO. In Fig. 10, the same performance behaviour is presented by range error mean graphs with a MIMO leading a SISO. Both curves display a similar trend to the simulation result. The averaging of beat signal spectrums was proven to increase the signal energy and improve range estimation accuracy.
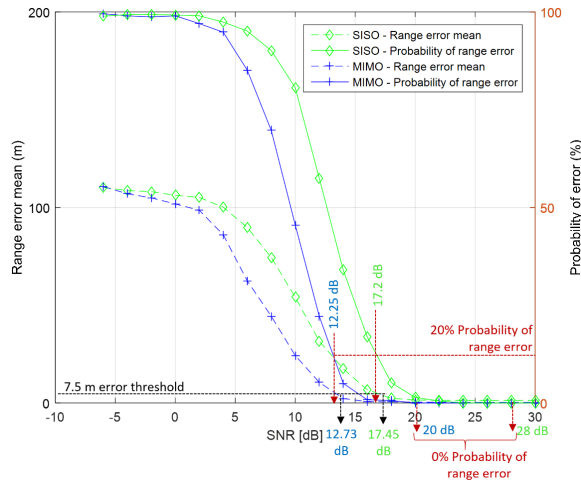
**Fig. 10. The effects of implementing a MIMO
FMCW with the spectrum averaging scheme.**

4.2. The effect of introducing more MIMO nodes

Next, the effect of nodes expansion in a MIMO configuration is presented in Fig. 11. The performance of a 3×3 MIMO was compared against a 2×2 MIMO for a single node, experimentally. The evaluation was carried out over a single MIMO node because of limited modules. For a single node, a 2×2 setup consisted of 2 beat signals, while a 3×3 setup consisted of 3 beat signals.

A setup with more nodes produced the 20% range error probability at 12.38 dB, followed by a lesser node setup at 13.53 dB. A 3×3 MIMO preceded a two-node configuration by 2 dB in delivering the 0% probability of range error, at 20 dB. Also, the improvement of range error mean by a three-node MIMO can be observed when the curve achieved average error within a threshold at 13.1 dB. It was followed by a configuration with two nodes MIMO at 14.02 dB. The result indicated improvement in the accuracy of target estimation, and more reliable detection could be achieved by having more frequency spectrums.
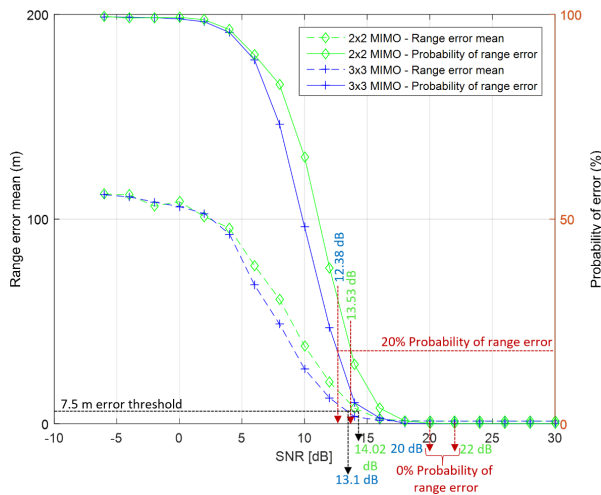

**Fig. 11. The effect of more MIMO node
configuration (evaluated for one receiver processing).**

4.3. The effect of interval band implementation

The effect of the proposed interval band scheme is demonstrated in Fig. 12. The experiment was conducted using 2×2 MIMO radar, with and without a 2 MHz interval band between sub-bands. From the figure, both configuration errors reduce sharply between 5 dB to 15 dB. Besides, the interval band implementation leads slightly for the probability of range error compared to a setup without an interval band. A setup with frequency interval delivered the 20% range error probability at 11.75 dB, whereby a setup without interval band was delivered at 12.25 dB.
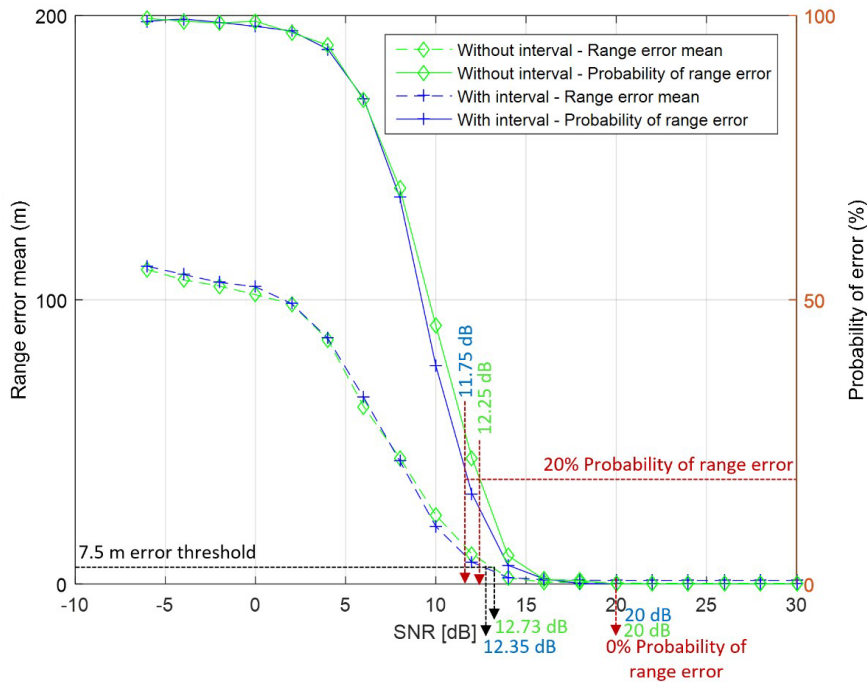

Fig. 12. The effects of 2 MHz interval band implementation.

A similar trend was observed for the range error mean, in which a setup with the proposed scheme produced an average error within the acceptable threshold started at 12.35 dB. Meanwhile, the other setup produced the same performance at 12.73 dB. The slight improvement in the trend was almost similar to moving target simulation. This may be due to clutter caused by the water surface that was not include during simulation.

5. Conclusions

An investigation was conducted on the proposed schemes' effects, a MIMO with multi-frequency triangular FMCW applying spectrum averaging and interval band. Effects were observed through numerical simulation and experimental evaluation on a small slow fluctuating target. Overall, experiment results presented slight degradation compared to simulation contributable from the clutter by the water surface and surrounding which did not include in the simulation.

Some concluding observations from the investigation are given below.

- Implementation of spectrum averaging increases the signal energy, which outweighs noise at the MIMO receiver and produces better range estimation accuracy.
- By increasing the number of nodes in MIMO, the range error estimation can be reduced by having more reliable and dependent signal sources for target estimation. However, it increases the computational cost of the system.
- Implementation of interval band prevents the interference and overlapping between sub-bands.
- By implementing interval band in MIMO FMCW sub-bands with the SA processing, better accuracy is produced, and error performance can be reduced.

Nomenclatures

B	Sweep bandwidth, Hz
BW	Baseband frequency range, Hz
c	Constant for velocity of light, 3×10^8 m/s
f_b	Beat frequency, Hz
f_c	Carrier frequency/ Operating frequency, Hz
f_s	Sampling frequency, Hz
M	Number of transmitting antennas
N	Number of receiving antennas
N_s	Number of samples
P_{ave}	Spectrum averaging output, log magnitude
P_k	FFT magnitude of k beat signal FFT, log magnitude
T	Sweep period, sec

Greek Symbols

ΔR	Maximum range estimation error
Δr	Range resolution, m

Abbreviations

COTS	Commercially off-the-Shelf
D2G	Distance2Go
DVB-T	Digital Versatile Broadcasting - Television
FFT	Fast Fourier Transform
FMCW	Frequency Modulated Continuous Waveform
FSPL	Free Space Path Loss
MIMO	Multiple-Input Multiple-Output
PVC	Polyvinyl Chloride
RCS	Radar Cross Section
RUT	Radar Under Test
SA	Spectrum Averaging
SAR	Synthetic Aperture Radar
SISO	Single-Input Single-Output
SNR	Signal to Noise Ratio

References

1. Hinz, J.O.; and Zölzer, U. (2011). A MIMO FMCW radar approach to HFSWR. *Advances in Radio Science*, 9, 159-163.

2. International Association of Marine Aids to Navigation and Lighthouse Authorities (2015). *Preparation of operational and technical performance requirements* (1st *ed.*), France.

3. Swerling, P. (1954). *Probability of detection for fluctuating targets*. U.S. Airforce, Project RAND, Research Moemorundum, Santa Monica.

4. Skolnik, M. (1999). Introduction to radar systems. (3rd ed.). McGraw-Hill Education.

5. McDonald, M.; and Balaji, B. (2008). Track-before-detect using swerling 0,1, and 3 target models for small manoeuvring maritime targets. *EURASIP Journal on Advances in Signal Processing*, 326259.

6. Kabakchiev, H.; Behar, V.; Garvanov, I.; Kabakchieva, D.; Daniel, L.; Kabakchiev, K.; Gashinova, M.; and Cherniakov, M. (2015). Experimental verification of maritime target parameter evaluation in forward scatter maritime radar. *IET Radar*, *Sonar & Navigation*, 9(4), 355-363.

7. Laghezza, F.; Scotti, F.; Serafino, G.; Banchi, L.; Malaspina, V.; Ghelfi, P.; and Bogoni, A. (2015). Field evaluation of a photonics-based radar system in a maritime environment compared to a reference commercial sensor. *IET Radar*, *Sonar & Navigation*, 9(8), 1040-1046.

8. Scotti, F.; Laghezza, F. ; Bogoni, A.; and Onori, D. (2015). Photonics-based dual-band radar demonstration for maritime traffic detection. *Proceddings of* 2015 *International Topical Meeting on Microwave Photonics* (*MWP*), Paphos, Cyprus, 1-4.

9. Stastny, J. ; Cheung, S.; Wiafe, G.; Agyekum, K.; and Greidanus, H. (2015). Application of RADAR corner reflectors for the detection of small vessels in synthetic aperture radar. *IEEE Journal of Selected Topics in Applied Earth Observations and Remote Sensing*, 8(3), 1099-1107.

10. Vieira, F.M.; Vincent, F.; Tourneret, J.-Y.; Bonacci, D.; Spigai, M.; Ansart, M.; and Richard, J. (2016). Ship detection using SAR and AIS raw data for maritime surveillance. *Processing of* 2016 24*th European Signal Processing Conference* (*EUSIPCO*), Budapest, Hungary, 2081-2085.

11. Ummenhofer, M.; Schell, J.; Heckenbach, J.; Kuschel, H.; and D'O Hagan, D.W. (2015). Doppler estimation for DVB-T based passive radar systems on moving maritime platforms. *Proceedings of* 2015 *IEEE Radar Conference* (*RadarCon*), Arlington, VA, USA,1687-1691.

12. Gierull, C.H. (2019). Demystifying the capability of sublook correlation techniques for vessel detection in SAR imagery. *IEEE Transactions on Geoscience and Remote Sensing*, 57(4), 2031-2042.

13. Daniel, L.; Hristov, S.; Lyu, X.; Stove, A.G.; Cherniakov, M.; Gashinova, M. (2017). Design and validation of a passive radar concept for ship detection using communication satellite signals. *IEEE Transactions on Aerospace and Electronic Systems*, 53(6), 3115-3134.

14. Johansen. T.A.; and Perez, T. (2016). Unmanned aerial surveillance system for hazard collision avoidance in autonomous shipping. *Proceedings of* 2016

International Conference on Unmanned Aircraft Systems (*ICUAS*), Arlington, VA, USA, 1056-1065.

15. Pasya, I.; Iwakiri, N.; and Kobayashi, T. (2014). Joint direction-of-departure and direction-of-arrival estimation in a UWB MIMO radar detecting targets with fluctuating radar cross sections. *International Journal of Antennas and Propagation*, Volume 2014 | Article ID 847815, 277-280.

16. FMCW vs. Pulse Radar (2019). What is the difference between frequency modulated continuous-wave (FMCW) and pulsed wave or pulsed width radar? Retrieved April 16, 2020, from https://www.automation.com/getattachment/ d201a032-1c4b-4885-b41b-b2c0400b3cd2/FMCW-vs-Pulse-Radar-White-Paper.pdf?lang=en-US&ext=.pdf.

17. Suryana, J.; and Ridha, M. (2016). Design and implementation of S-Band MIMO FMCW radar. Proceedings of 2016 10*th International Conference on Telecommunication Systems Services and Applications* (*TSSA*), Denpasar, Indonesia, 1-5.

18. Zainuddin, S.; Pasya, I.; Abd Rashid, N.E.; Raja Abdullah, R.S.A..; and Abdullah, A.R. (2018). Performance of MIMO FMCW radar in detecting small vessels. *Proceedings of* 2018 *IEEE* 2018 *IEEE International RF and Microwave Conference* (*RFM*), Penang, Malaysia, 329-332.

19. Md Noor, A.M.; Pasya, I.; Abd Rashid, N.E.; and Raja Abdullah, R.S.A. (2020). MIMO FM-CW radar using beat signal averaging method. *Proceedings of* 2020 *International Workshop on Antenna Technology* (*iWAT*), Bucharest, Romania, 1-3.

20. Frischen, A. ; Hasch, J.; and Waldschmidt, C. (2017). A cooperative MIMO radar network using highly integrated FMCW radar sensors. *IEEE Transactions on Microwave Theory and Techniques*, 65(4), 1355-1366.

21. Choi, M.G.; Woo, D.S.; Choi, H.C.; and Kim, K.W. (2017). High-accuracy am-fm radar with an active reflector. *Journal of Sensors*, Volume 2017 | Article ID 8589469, 1-9.

22. Signal processing toolbox (2020). Signal processing toolbox - fir1. Retrieved April 16, 2020, from http://matlab.izmiran.ru/help/toolbox/signal/fir1.html.

23. Algorithm Time Cost Measurement. (2020). Retrieved April 28, 2020, from http://cseweb.ucsd.edu/~kube/cls/12.s13/Lectures/lec06/lec06.pdf.

24. Yu, X.; Chen, X.; Huang, Y.; Zhang, L.; Guan, J.; and He, Y. (2019). Radar moving target detection in clutter background via adaptive dual-threshold sparse Fourier transform. *IEEE Access*, 7, 58200-58211.